# Impacts of land-use change on Sydney's future temperatures

**Matthew Adams, Hiep Duc and Toan Trieu**

# Contents

# List of figures

## List of tables

# 1.  Introduction

Cities create their own microclimates through influencing the surrounding atmosphere and interacting with climate processes. The most striking characteristic of an urban microclimate is the urban heat island (UHI) effect. The UHI effect results in higher air temperatures in urban areas (2–5°C higher on average but in some cases more than 10°C higher) than those in surrounding non-urban areas (Taha 1997). In Sydney, morning summer surface temperatures in treeless urban areas are on average 12.8°C higher than treed non-urban areas (Adams & Smith 2014). This phenomenon is expected to increase in Sydney due to a growing majority of the NSW population residing in urban areas. According to Taylor et al. (2014), in the years 2011–31 Sydney's population is expected to rise by over 1.5 million (37%). This population increase is expected to lead to an increase in households of 600,000 (40%). By mid-century, global average temperatures are projected to rise by 0.9–2.6°C in response to unmitigated anthropogenic greenhouse warming (IPCC 2013). Given this, many people in NSW may be exposed to average maximum temperatures several degrees warmer than those currently experienced in adjacent rural areas today.

Planners and policy-makers are looking at different ways to alleviate expected temperature increases. Global and regional climate model projections give a good basis for planners and policy-makers to prepare for such future climate changes. In NSW, information derived from climate model projections has been incorporated into government planning on risks such as bushfires, coastal inundation and water security. However, the coarse resolution of most models (10–300 km grid cells) does not allow us to accurately define an urban microclimate and the UHI effect (Chen et al. 2004; Pielke 2002). Urban microclimates are better determined by climate model projections that have a fine scale (e.g. 1 km grid cells) (Chen et al. 2011). Other than a fine scale resolution, Jackson et al. (2010) determined that climate models required three categories of input parameters to effectively simulate the urban influences on climate: 1) spatial extent of urban areas, 2) urban morphology characteristics, i.e. building density and structure, and 3) accurate urban canopy parameters. Major urban canopy parameters include vegetation cover fraction, building height and cover fraction, industrial sensible heat flux, albedo, emissivity and soil variables. In addition, temporal changes to land cover, such as urban expansion and increased urban density, should also be accounted for, as they can lead to a significantly different climate when compared with climate resulting from atmospheric forces alone (Feddema et al. 2005).

The objective of this study was to create fine scale (1 km) urban temperature projections for the Sydney greater metropolitan area (GMA) and assess the extent to which anticipated changes in land-use may affect future temperature projections for the region. Dwelling densities based on land-use data are used to more accurately depict current and future urban extent and structure than those typically used in global and regional climate modelling. The projections use up to date urban canopy parameters based on Australian cities. The projections illustrate the impact of urban development and increased population density on temperature within Sydney's GMA.

# 2. Data and methods

The NSW and ACT Regional Climate Modelling (NARCliM) project provides robust climate change projections for South-East Australia (SEA) at a scale relevant for local-scale impact studies. In NARCliM, simulations from four global climate models (GCMs) were used to drive three regional climate models (RCMs) to form a 12-member GCM/RCM ensemble (Evans et al. 2014). The four selected GCMs are MIROC3.2, ECHAM5, CCCMA3.1 and CSIRO-MK3.0. For the future projections the SRES A2 emissions scenario was used. The three selected RCMs are three physics scheme combinations of the Weather Research Forecast (WRF) model. Each simulation consists of three 20-year runs, a base case period 1990–2009, near future period 2020–2039, and far future period 2060–2079). The four GCMs and three RCMs were chosen based on a number of criteria: i) adequate performance when simulating historic climate; ii) most independent; iii) cover the largest range of plausible future precipitation and temperature changes for Australia (only for selection of GCMs). NARCliM outputs climate projection data at 50 km resolution for Australasia and 10 km resolution for SEA, and for 30 vertical levels spaced closer together in the planetary boundary layer.

In this study we created fine scale (1 km) urban temperature projections for the Sydney GMA based on the 50 km ECHAM5 GCM-driven RCM (R3) simulations. ECHAM5 was selected due to this GCM projecting the greatest increases in temperatures, providing the study with a conservative (upper bound) estimate of temperature increases. R3 was chosen as it most accurately depicts observed temperatures for SEA for the base case period, 1990–2009 (Ji et al. 2015). Based on the ECHAM5 GCM-driven RCM (R3) simulations from the NARCliM project, average annual temperature for the Sydney GMA is projected to increase 0.8°C by 2020–2039 (when compared with the 1990–2009 base climate). Average seasonal temperatures are projected to increase by 1.2°C, 0.8°C, 0.5°C and 0.6°C for summer, autumn, winter and spring, respectively.

For this study the 50 km ECHAM5-R3 projections were dynamically downscaled using The Air Pollution Model (TAPM) to project recent and near future temperatures for the Sydney GMA. More accurate land-use data was used to depict current and future urban extent and structure than were used in NARCliM. Future temperatures were projected based on current and anticipated changes in urban land-use to illustrate the impact of urban sprawl and increased density on temperature within Sydney's GMA.

## 2.1 Study area

The city of Sydney and its GMA is located on the south-east coast of Australia. In this study, Sydney's GMA is defined as latitude –34° 18' 17" to –33° 25' 49", and longitude 151° 29' 39" to 150° 24' 11" (Figure 1). The GMA covers 64% of NSW's population. The climate is temperate with mild winters and warm summers.

**Figure 1: Sydney's greater metropolitan area (GMA)**

## 2.2 Methods

### 2.2.1 Land-use layers

WRF and TAPM simulate the urban influences on climate through the Noah land surface model and TAPM land surface model, respectively. Land-use types for both land surface models are defined by the Global Land Cover Characterisation Dataset layer (1 km resolution) from the US Geological Survey (Loveland et al. 2000; Hurley 2008). Each land-use type has a set of distinct parameters that influence climate for that particular land-use, e.g. forest, grassland, desert. However the dataset layer represents urban land-use with only a single generic urban category. Despite its single category default, TAPM supports multiple urban categories. In order to account for urban microclimates, in this study we divided Sydney's urban areas into five types: industrial/commercial, low density, medium density, high density, and CBD density. To represent current and future urban land-use more accurately, we use occupied dwelling data and projected changes from the Bureau of Transport Statistics (2012). The Bureau of Transport Statistics also provides projections of occupied dwelling data. To test the effects of these projected changes in land-use, we compare a present and a future land-use layer based on 2006 and 2036 occupied dwelling data respectively. Land-use layers were created using ARCMap. The 2006 occupied dwelling data was chosen as it is the most current data that falls within the NARCliM base case period

(1990–2009). Based on results from Cardew (1996), dwelling density (per square km) for each urban type is as follows: low (3–9), medium (10–15), high (16–50), CBD (50+). Industrial commercial sites were defined by the NSW land-use spatial layer obtained from the Office of Environment and Heritage Spatial Data Online Access database (OEH 2012) and added to the present and future land-use layers. The Global Land Cover Characterisation Dataset layer land-use types were used for areas with dwelling densities below three, with the exception of industrial/commercial sites. Industrial/commercial sites with a low dwelling density (such as the commercial area of the CBD and Kingsford-Smith Airport) were extracted from the land-use spatial layer and confirmed with dwelling data. No new industrial/commercial areas were added to the future land-use layer (for example, the planned airport at Badgerys Creek). Any area classified as urban according to the Global Land Cover Characterisation Dataset layer that has a dwelling density less than three and is not industrial or commercial, was replaced with surrounding non-urban classification values. Once complete the present and future land-use layers were resampled to a 1 km grid (Figure 2).
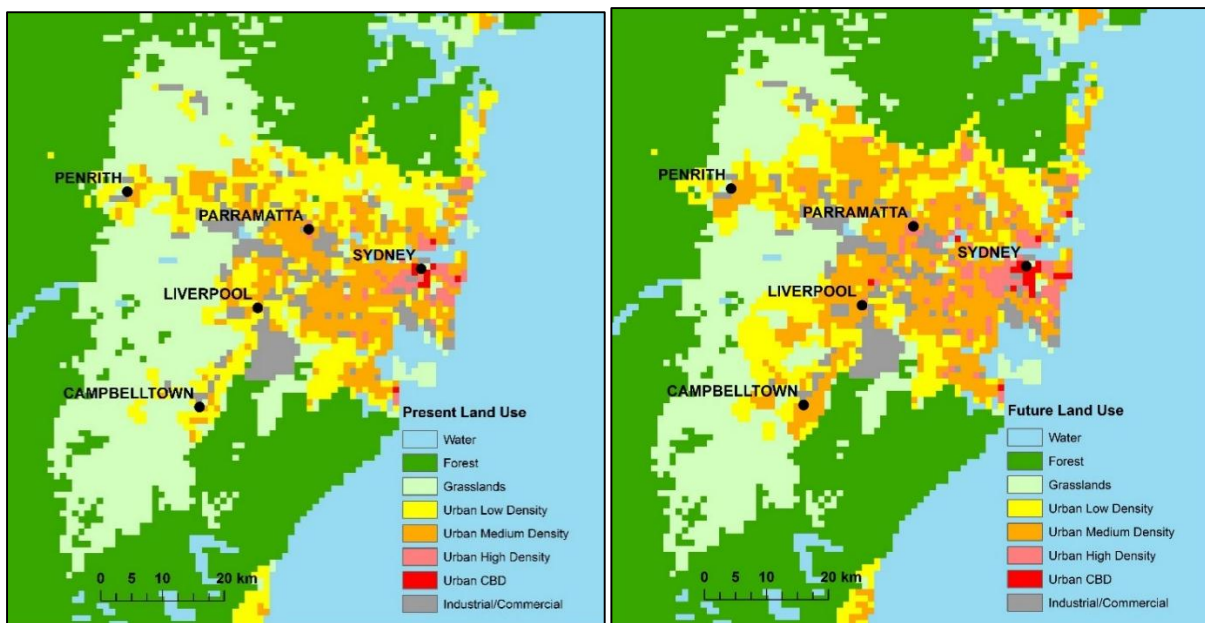


**Figure 2:  Present and future land-use layers for Sydney's urban region**

## 2.2.2  Urban canopy models

The default TAPM urban canopy model (UCM) is based on parameters established in Oke (1988) and Pielke (2002). For this study we incorporated changes to building and composition UCM parameters based on Lipson (2014) and Thatcher and Hurley (2012). Urban land-use types varied in the UCM by fraction of urban cover, fraction of building cover, building height, building height/width ratio and industrial sensible heat flux (Table 1).

**Table 1: Urban canopy model parameters**

| Land-use types | Fraction of urban cover | Fraction of building cover | Building height (m) | Building height / width ratio | Sensible heat flux industrial |
|---|---|---|---|---|---|
| Low density | 0.55 | 0.40 | 4 | 0.2 | 0 |
| Medium density | 0.62 | 0.45 | 6 | 0.4 | 0 |
| High density | 0.66 | 0.46 | 8 | 0.6 | 0 |
| CBD density | 0.95 | 0.65 | 18 | 2.0 | 0 |
| Industrial / commercial | 0.60 | 0.40 | 4 | 0.5 | 10 |

### 2.2.3 Meteorology

TAPM 4.0 was used to downscale the WRF model 50 km resolution synoptic data from the NARCliM project (Evans et al. 2014). A resolution of 50 km was used due to TAPM resolution input requirements. The data was downscaled to a 1 km resolution nested domain covering the Sydney GMA. The dimensions of the domain are 100 by 100 grid cells. Raw WRF 50 km synoptic data was converted to a TAPM-compatible format using the NCAR command language (NCL).

For the Sydney GMA domain, two future TAPM simulations of air temperature for the year 2036 were created using the present (2006) and future (2036) land-use layers. Seasonal hourly average temperatures projected for 2036 based on present and future land-use layers were extracted from TAPM and compared spatially using GIS. Summary comparison statistics were also created based on grid cells where land-use is projected to change between 2006 and 2036.

## 2.3 Limitations

For this study, accuracy of the model results is subject to the limitations imposed by the assumptions and parameterisations inherent in the NARCliM simulations and TAPM. This study will not model the NARCliM simulations' range of uncertainty in future climate, as only one of NARCliM's twelve member ensembles is used.

The land-use layers used in TAPM do not represent the full complexity of Sydney's urban surfaces. The 1 km resolution of the land-use layers requires averaged thermal and radiative surface properties, while the urban land-use categories average vegetation and building cover percentages. This study also does not account for future impact of changes in dwelling size or sites which have employed heat reducing strategies such as urban irrigation, high albedo materials and green walls and roofs.

# 3.  Results

## 3.1 Projected land-use changes

Over 11% or 734 km$^2$ of the Sydney GMA is projected to change land-use types between 2006 and 2036 based on the urban density categories used (Table 2). The projected changes were categorised into seven types of land-use change: forest to low or higher density urban (F→L+), grasslands to low density urban (G→L), grasslands to medium or higher density urban (G→M+), low density urban to medium or higher density urban (L→M+), medium density urban to high or CBD density urban (M→H+), high density urban to CBD density urban (H→C) and industrial/commercial to low density urban (I→U) The two largest changes will be the conversion of grasslands to low density urban (229 km$^2$) and low density urban to urban land-uses with higher densities (306 km$^2$).

**Table 2:   Number and type of projected land-use changes**

| Present land-use | Future land-use | No. of cell changes | Abbreviation |
|---|---|---|---|
| All types | No change | 9,266 | None |
| Forest | Low density urban (+) | 35 | F → L+ |
| Grasslands | Low density urban | 229 | G → L |
| Grasslands | Medium density urban (+) | 77 | G → M+ |
| Low density urban | Medium density urban (+) | 306 | L → M+ |
| Medium density urban | High density urban (+) | 69 | M → H+ |
| High density urban | CBD density urban | 8 | H → C |
| Industrial / commercial | Low density urban (+) | 10 | I → U |

Note: (+) includes urban land-uses with higher densities

Figure 3 spatially illustrates projected land-use changes by 2036 for the GMA. Changes from one urban category to another are spread throughout the present urban area. Not surprisingly H→C changes will occur around Sydney city and the surrounding coast line. M→H+ changes will occur across much of the present urban area. These changes are projected to occur in areas up to 40 km west of the Sydney CBD in large town centres such as Parramatta, Hornsby, Liverpool and Blacktown. L→M+ changes are predominantly projected to occur at the outskirts of the existing urban extent and along major arterial roads (M4 and M5). The majority of the G→L changes will occur in relatively large areas of existing grasslands identified for suburban development in the North-West and South-West Priority Growth Areas of the present urban extent. F→L+ changes will encroach on forested areas in the Blue Mountains in the west and across most of the north of the present urban extent.
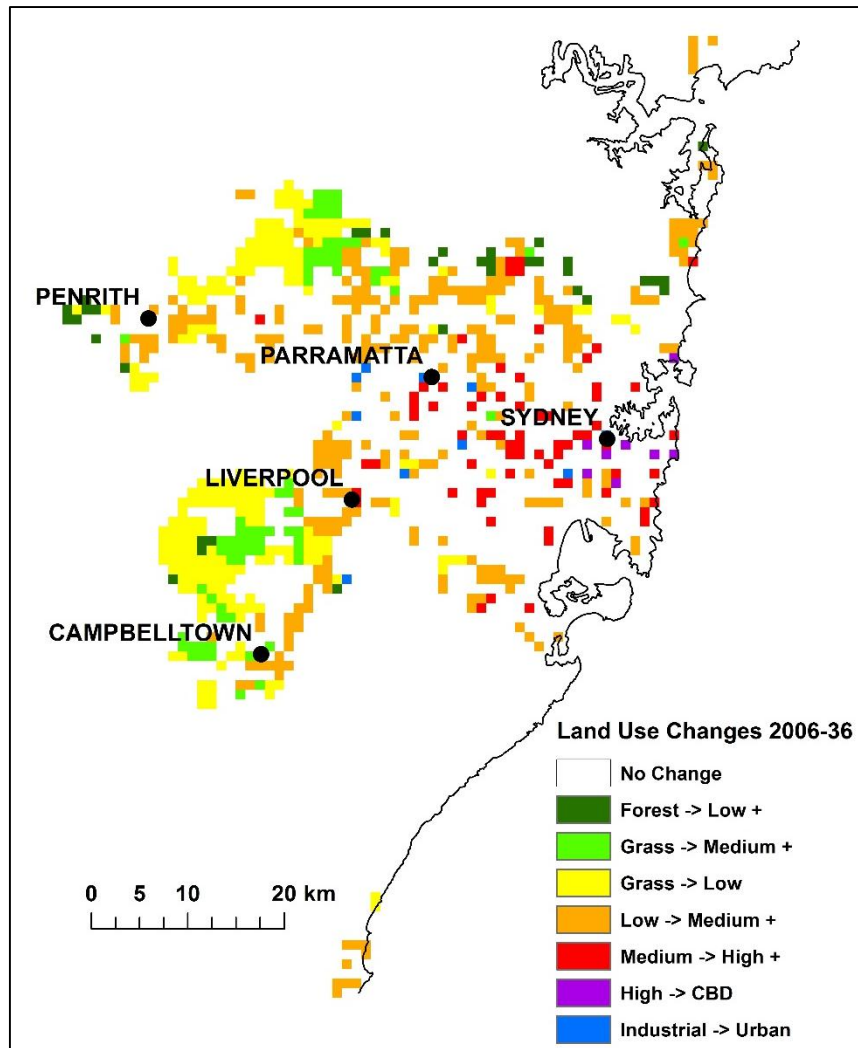
**Figure 3:** **Projected changes in land-use by 2036**

## 3.2 Annual temperature changes

Annual average hourly temperature changes range from –1.3 to +1.4°C. Annual average daily temperature changes range from –0.4 to +0.8°C. On average, annual temperatures will increase in areas which are converted from forest or grasslands to urban (F→L+, 0.3°C; G→L, 0.2°C; G→M+, 0.4°C) and from low urban density to higher urban density (L→M+, 0.1°C). Medium and high density urban areas projected to increase in density will have lower average temperatures, –0.1°C and –0.2°C respectively. Where industrial/commercial land-use changes to low density urban, temperatures on average will not change. Figure 4 illustrates 3-hourly temperature changes for projected land-use changes.

**Annual temperature changes**



**Figure 4:   Average 3-hourly annual temperature changes for projected land-use changes**

Figure 5 and Figure 6 show how land-use changes are projected to influence future annual temperatures throughout an average day. Between the hours of 1 am and 6 am very sparse and relatively low changes in temperature are projected to occur. Between 7 am and 9 am, a slight increase in temperature covers most of the future urban extent. Between 10 am and 12 pm the coverage expands and is speckled with larger increases. The locations of the larger increases match cells where forests are converted to urban, industrial/commercial is converted to low density urban, and where some low urban density to higher urban density changes occur. In the afternoon temperature is further increased in areas where urban land-use has replaced forest and grasslands. Large areas of the GMA to the south-west and north-west are projected to have temperature increases of 1–1.4°C due to these land-use changes. Suburbs in these areas include Oran Park, Leppington, Catherine Fields, Marsden, Riverstone and Vineyard. Increased temperatures are projected for the night, beginning to dissipate between 10 pm and 12 am. During this time, a slight decrease will occur in coastal areas where higher density development is projected.
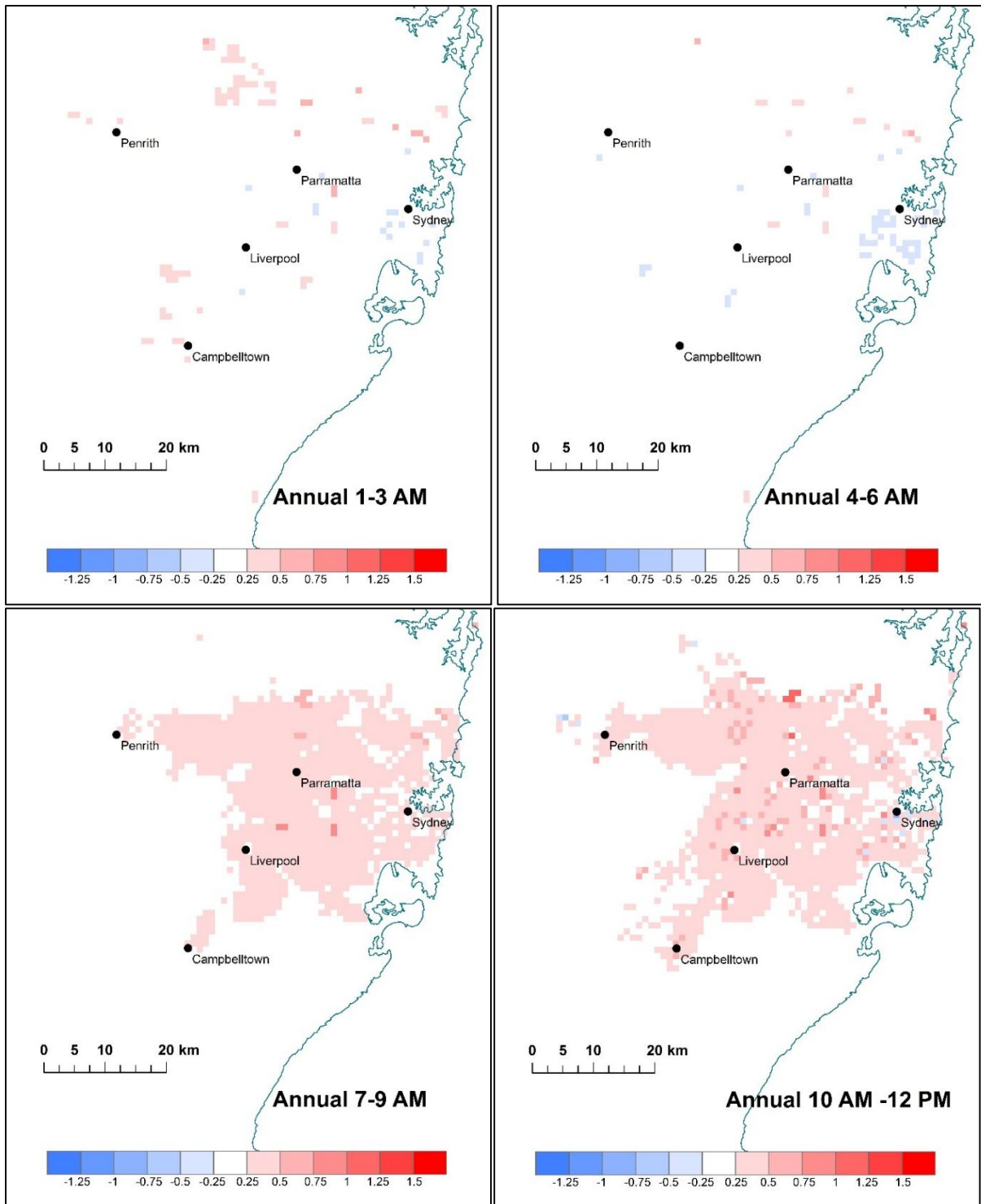
**Figure 5:  3-hourly annual temperature changes between 1 am and 12 pm**
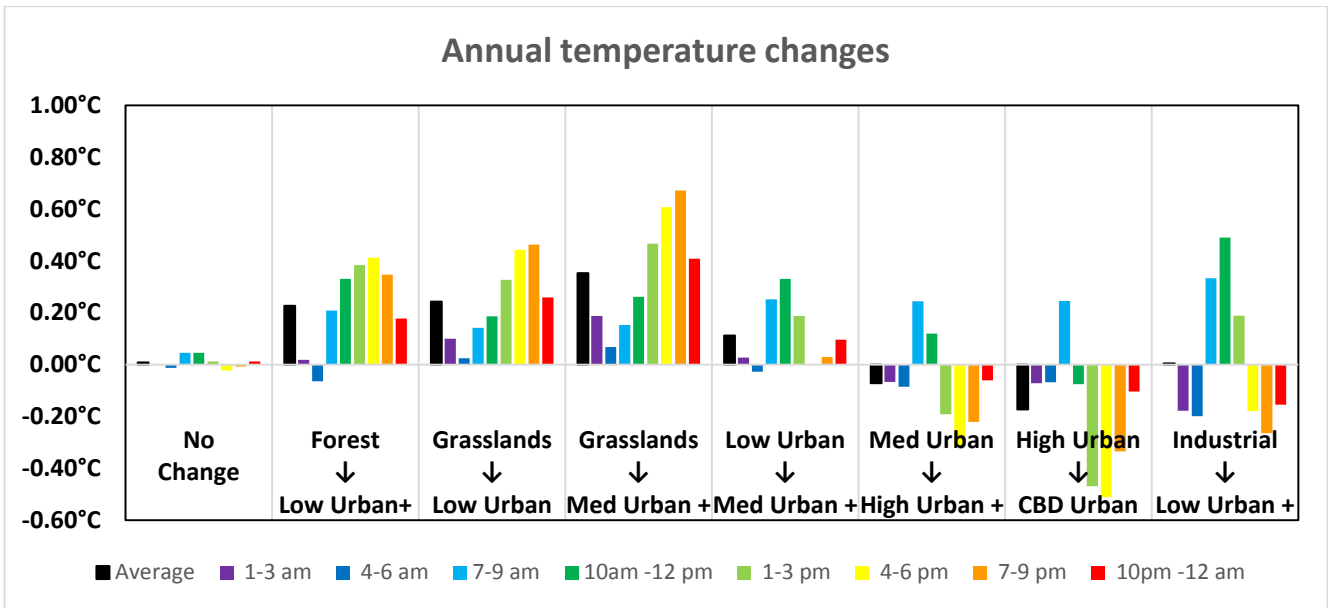
**Figure 6:   3-hourly annual temperature changes between 1 pm and 12 am**

## 3.3  Spring temperature changes

Spring average hourly temperature changes range from –1.7 to +1.5°C. Spring average daily temperature changes range from –0.5 to +0.8°C. On average, spring temperatures will increase in areas which are converted from forest or grasslands to urban (F→L+, 0.3°C; G→L, 0.3°C; G→M+, 0.4°C) and from low urban density to higher urban density (L→M+, 0.2°C). Medium and high density urban areas projected to increase in density will have lower average temperatures, –0.1°C and –0.2°C respectively. Where industrial/commercial land-

use changes to low density urban, temperatures on average will not change. Figure 7 illustrates 3-hourly temperature changes for projected land-use changes.



**Spring temperature changes**

Legend: Average | 1-3 am | 4-6 am | 7-9 am | 10am -12 pm | 1-3 pm | 4-6 pm | 7-9 pm | 10pm -12 am

**Figure 7:    Average 3-hourly spring temperature changes for projected land-use changes**

Figure 8 and Figure 9 show how land-use changes are projected to influence future spring temperatures throughout an average day. Between the hours of 1 am and 6 am very sparse and relatively low changes in temperature are projected to occur. Between 7 am and 9 am, a slight increase in temperature covers most of the future urban extent. Between 10 am and 12 pm the coverage expands and is speckled with larger increases. The locations of the larger increases match cells where forests are converted to urban, industrial/commercial is converted to low density urban, and where some low urban density to higher urban density changes occur. In the afternoon temperature is further increased in areas where urban land-use has replaced forest and grasslands. The Priority Growth Areas in the North-West and South-West are projected to have temperature increases of 1–1.5°C due to these land-use changes. Increased temperatures are projected for the night, beginning to dissipate between 10 pm and 12 am. During this time, a slight decrease will occur in coastal areas where higher density development is projected.

**Figure 8:  3-hourly spring temperature changes between 1 am and 12 pm**
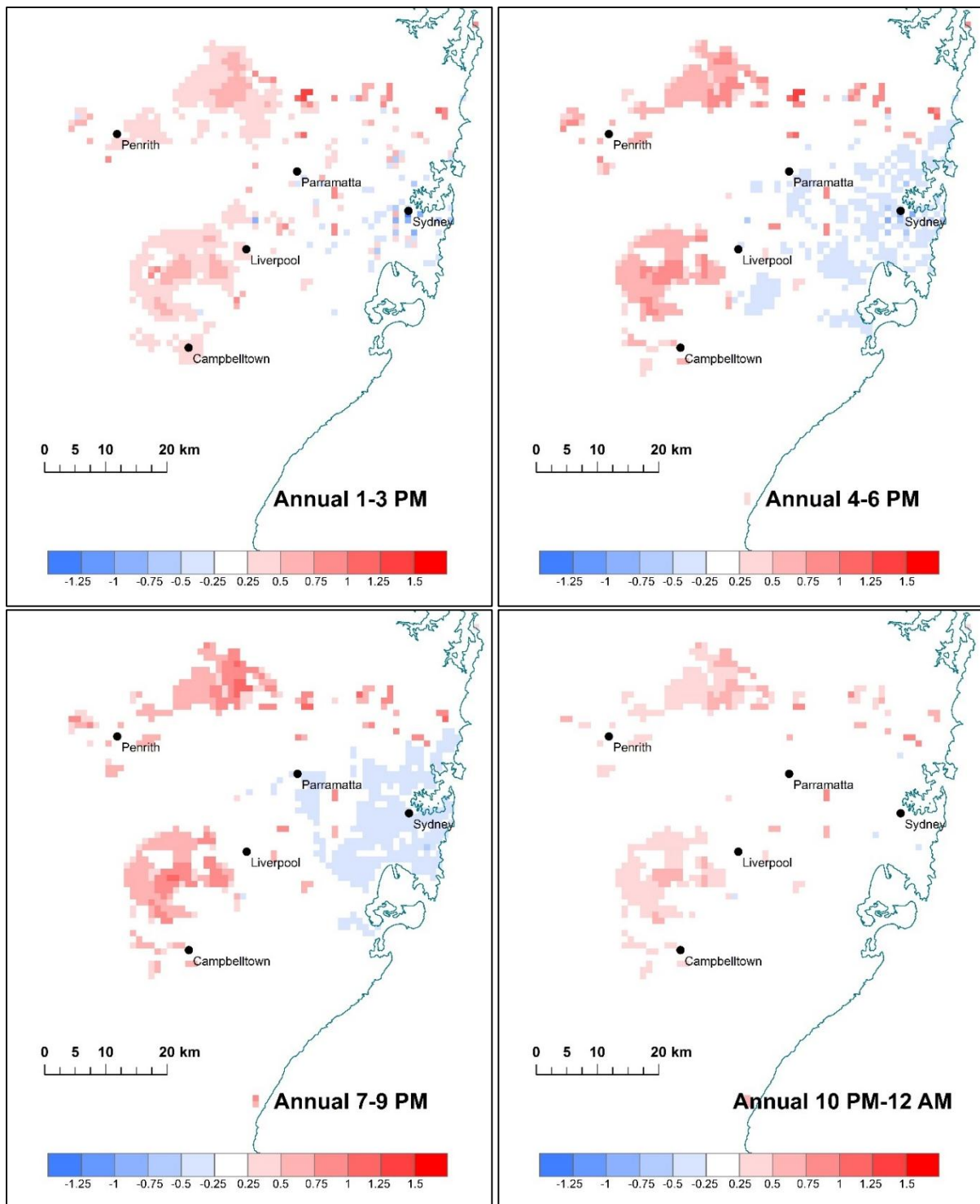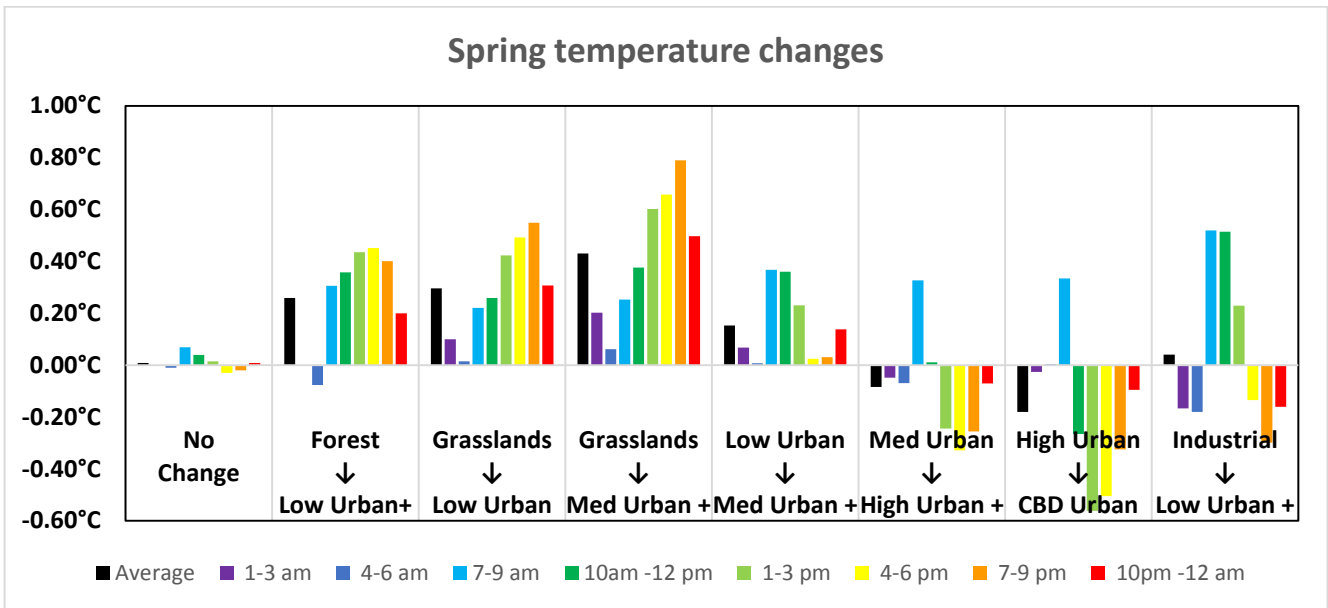
**Figure 9:  3-hourly spring temperature changes between 1 pm and 12 am**

## 3.4  Summer temperature changes

Summer average hourly temperature changes range from –1.4 to +1.8°C. Summer average daily temperature changes range from –0.5 to +1°C. On average, summer temperatures will increase in areas which are converted from forest or grasslands to urban (F→L+, 0.3°C; G→L, 0.3°C; G→M+, 0.5°C) and from low urban density to higher urban density (L→M+, 0.2°C). Medium and high density urban areas projected to increase in density will have lower average temperatures, –0.1°C and –0.2°C respectively. Where industrial/commercial land-

use changes to low density urban, temperatures on average will not change. Figure 10 illustrates 3-hourly temperature changes for projected land-use changes.

**Summary temperature changes**



**Figure 10: Average 3-hourly summer temperature changes for projected land-use changes**

Figure 11 and Figure 12 show how land-use changes are projected to influence future summer temperatures throughout an average day. Between the hours of 1 am and 6 am very sparse and relatively low changes in temperature are projected to occur. Between 7 am and 9 am, a slight increase in temperature covers most of the future urban extent. Between 10 am and 12 pm the coverage expands and is speckled with larger increases. The locations of the larger increases match cells where forests are converted to urban, industrial/commercial is converted to low density urban, and some where low urban density to higher urban density changes occur. In the afternoon temperature is further increased in areas where urban land-use has replaced forest and grasslands. The Priority Areas in the North-West and South-West are projected to have temperature increases of 1–1.8°C due to these land-use changes. The increased temperatures are projected for the night, beginning to dissipate between 10 pm and 12 am. However, higher temperatures will remain throughout the 24-hour period for large portions of these areas. During this time, a slight decrease will occur in coastal areas where higher density development is projected.

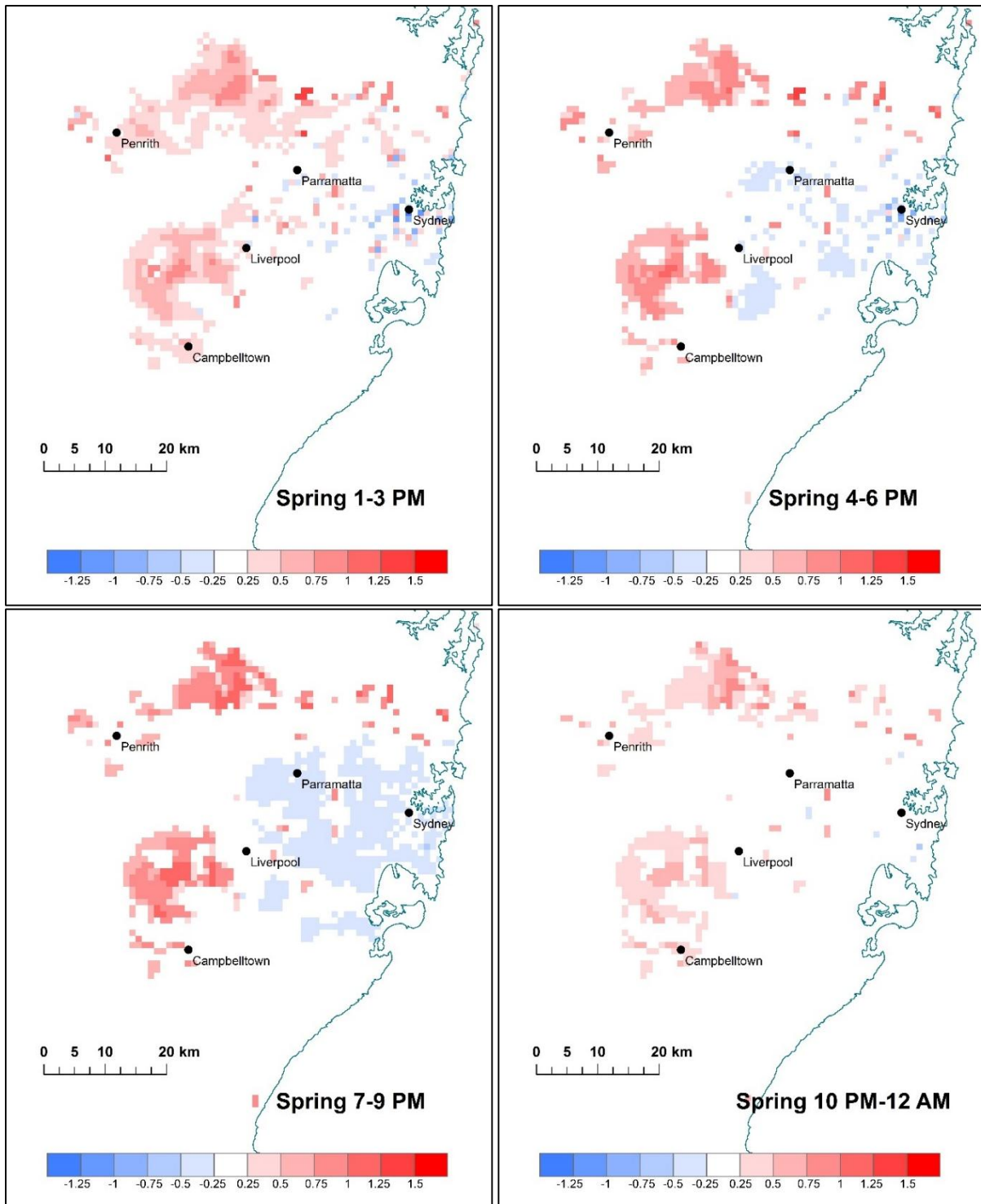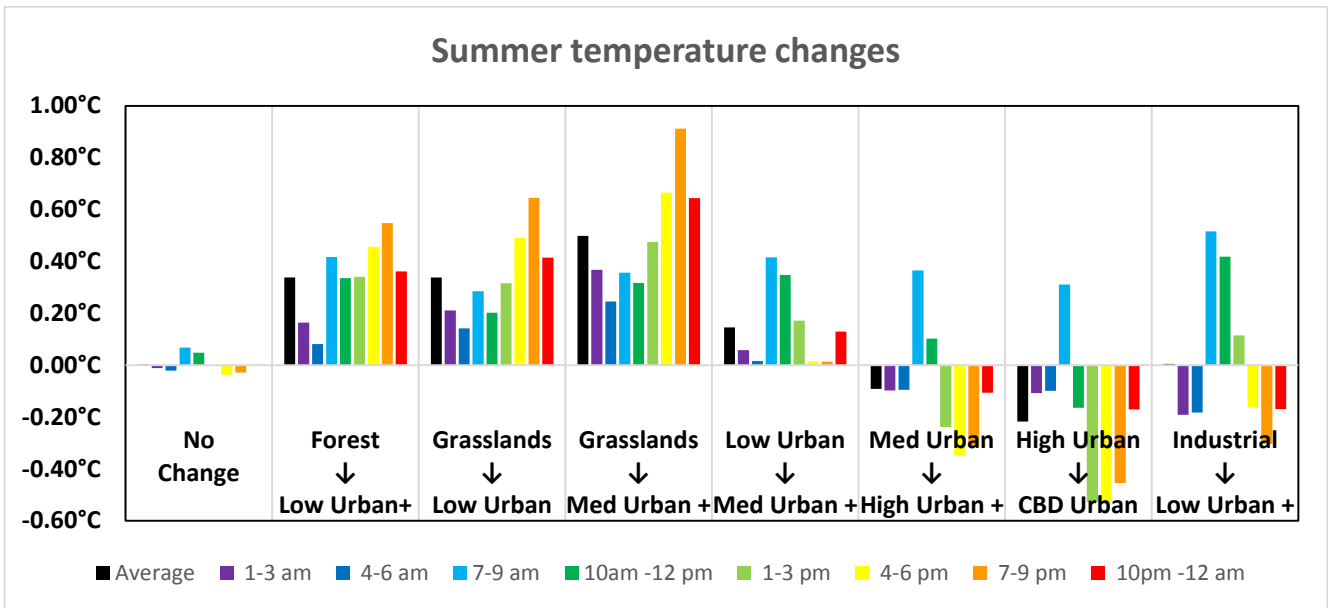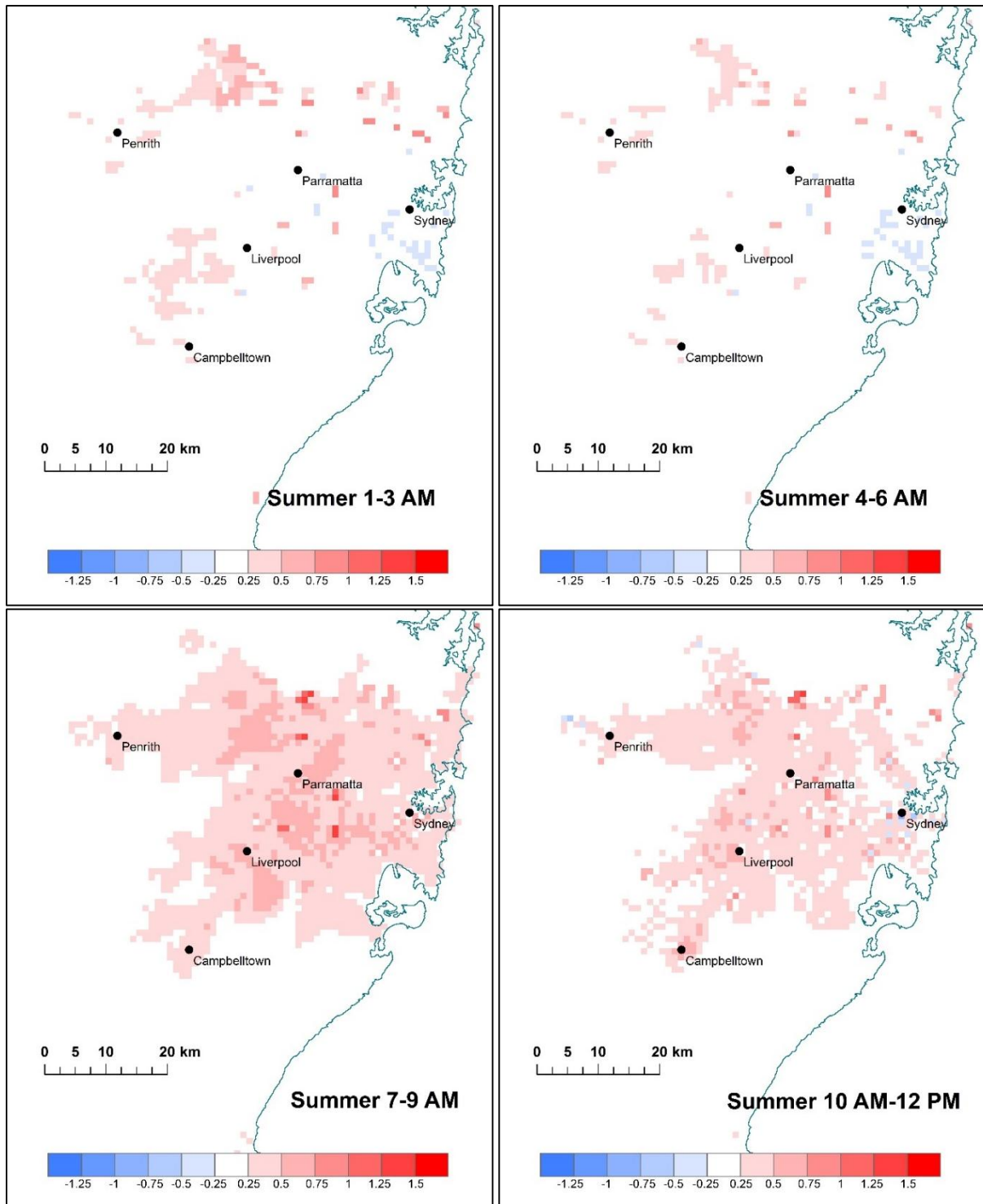**Figure 11: 3-hourly summer temperature changes between 1 am and 12 pm**

**Figure 12: 3-hourly summer temperature changes between 1 pm and 12 am**

## 3.5 Autumn temperature changes

Autumn average hourly temperature changes range from –1.3 to +1.5°C. Autumn average daily temperature changes range from –0.4 to +0.9°C. On average, autumn temperatures will increase in areas which are converted from forest or grasslands to urban (F→L+, 0.2°C; G→L, 0.2°C; G→M+, 0.3°C) and from low urban density to higher urban density (L→M+, 0.09°C). Medium and high density urban areas projected to increase in density will have lower average temperatures, –0.1°C and –0.2°C respectively. Where industrial/commercial

land-use changes to low density urban, temperatures on average will not change. Figure 13 illustrates 3-hourly temperature changes for projected land-use changes.
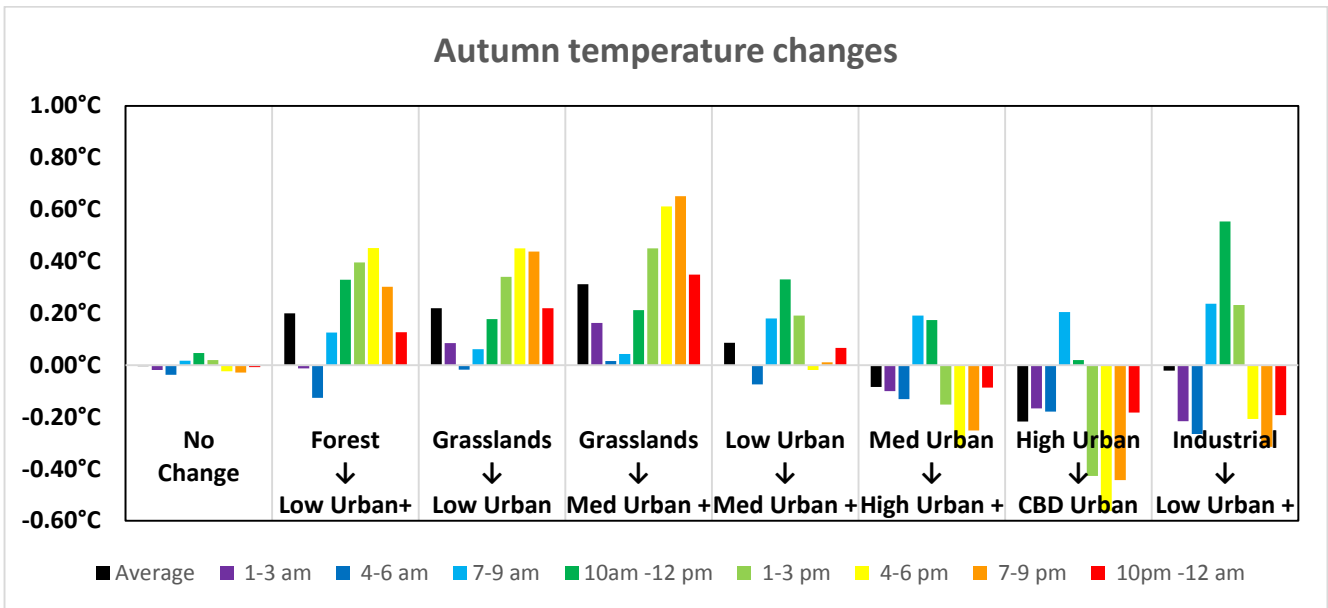


**Figure 13: Average 3-hourly autumn temperature changes for projected land-use changes**

Figure 14 and Figure 15 show how land-use changes are projected to influence future autumn temperatures throughout an average day. Between the hours of 1 am and 6 am very sparse and relatively low changes in temperature are projected to occur. Between 7 am and 9 am, a slight increase in temperature will cover a large portion of the western half of the future urban extent. Between 10 am and 12 pm the coverage expands to cover the entire extent and is speckled with larger increases. The locations of the larger increases match cells where forests are converted to urban, industrial/commercial is converted to low density urban, and where some low urban density to higher urban density changes occur. In the afternoon temperature is further increased in areas where urban land-use has replaced forest and grasslands. The Priority Growth Areas in the North-West and South-West are projected to have temperature increases of 1–1.5°C due to these land-use changes. Increased temperatures are projected for the night, beginning to dissipate between 10 pm and 12 am. During this time, a slight decrease will occur in coastal areas where higher density development is projected.

**Figure 14: 3-hourly autumn temperature changes between 1 am and 12 pm**
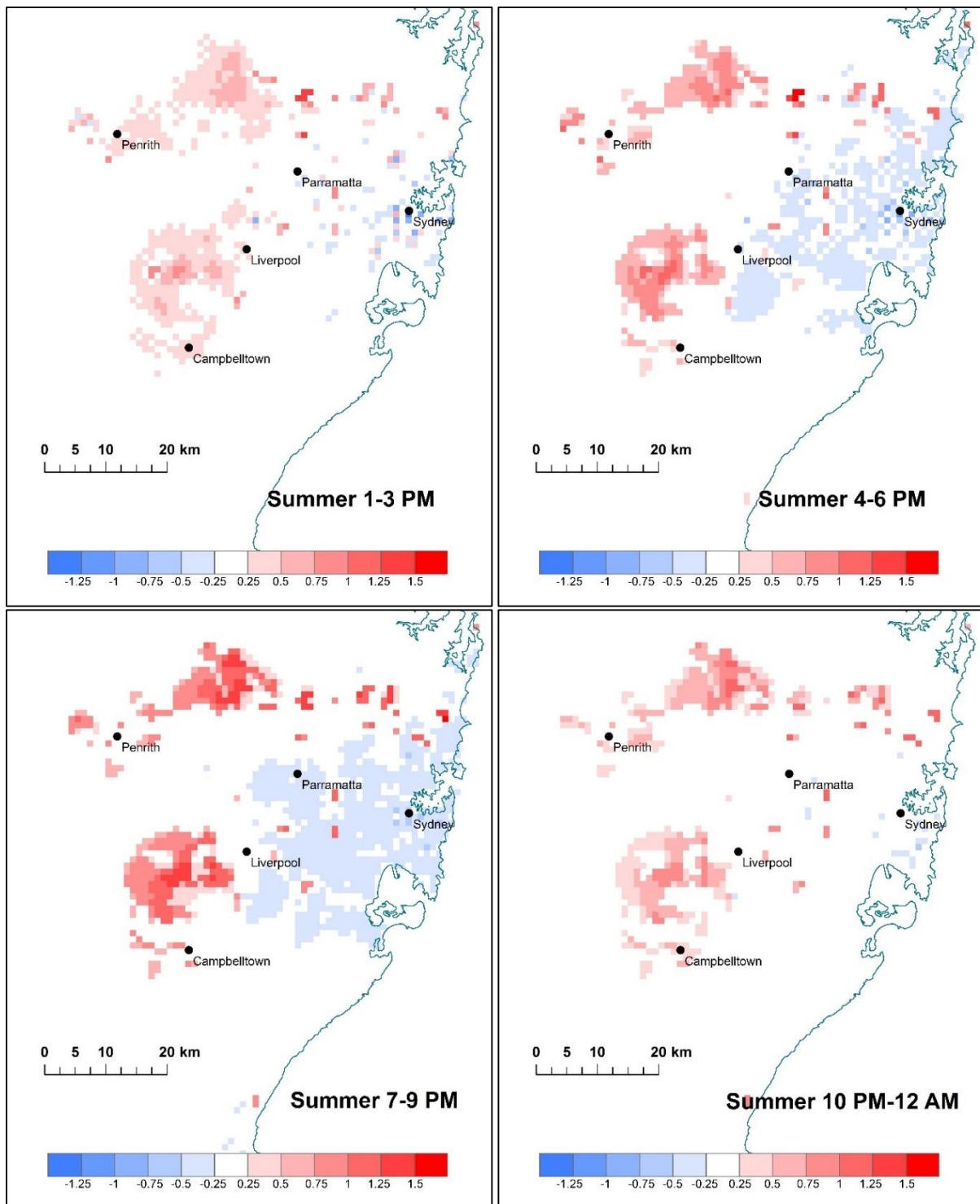
**Figure 15: 3-hourly autumn temperature changes between 1 pm and 12 am**

## 3.6 Winter temperature changes

Winter average hourly temperature changes range from –0.9 to +1.2°C. Winter average daily temperature changes range from –0.2 to +0.5°C. On average, winter temperatures will increase in areas which are converted from forest or grasslands to urban (F→L+, 0.1°C; G→L, 0.1°C; G→M+, 0.2°C) and from low urban density to higher urban density (L→M+, 0.1°C). High density urban areas projected to increase in density will have lower average temperatures (–0.1°C). Medium density urban areas projected to increase in density and

where industrial/commercial land-use changes to low density urban, temperatures on average will not change. Figure 16 illustrates 3-hourly temperature changes for projected land-use changes.
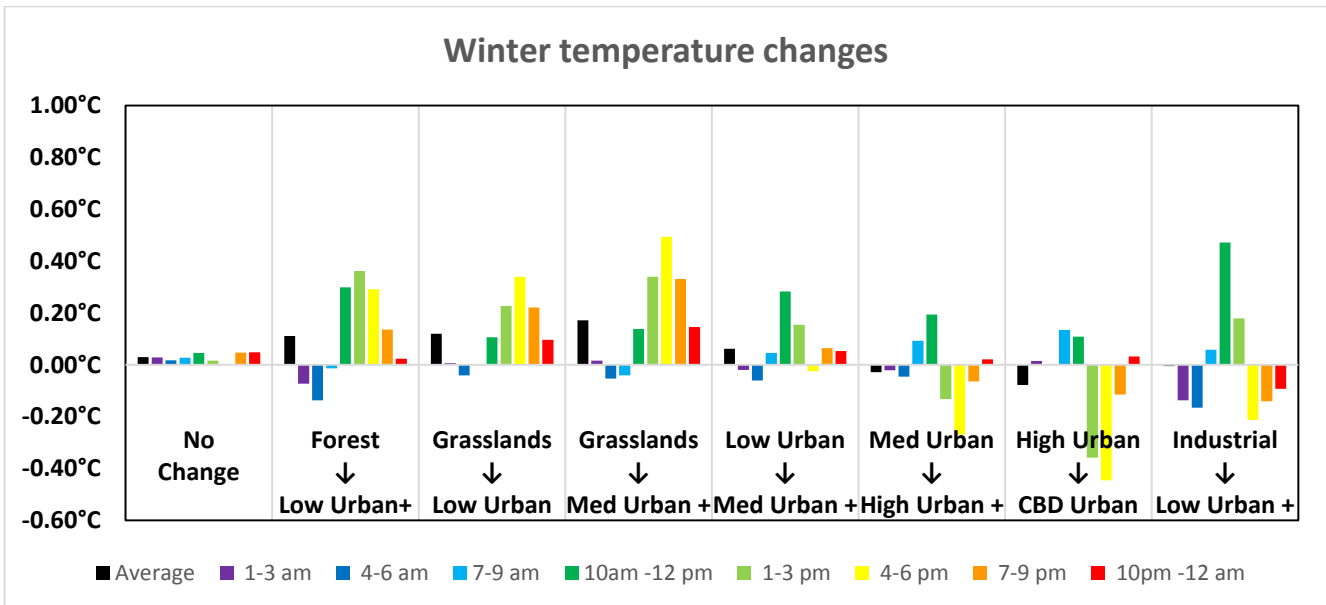


**Figure 16: Average 3-hourly winter temperature changes for projected land-use changes**

Figure 17 and Figure 18 show how land-use changes are projected to influence future winter temperatures throughout an average day. Between the hours of 1 am and 9 am almost no changes in temperature are projected to occur. Between 10 am and 12 pm, a slight increase in temperature covers most of the future urban extent and is speckled with larger increases. The locations of the larger increases match cells where forests are converted to urban, industrial/commercial is converted to low density urban, and some where low urban density to higher urban density changes occur. In the afternoon temperature is further increased in areas where urban land-use has replaced forest and grasslands. The Priority Growth Areas in the North-West and South-West are projected to have temperature increases of 0.5–1°C due to these land-use changes. Increased temperatures are projected for the night, beginning to dissipate between 7 pm and 9 pm. In addition, a slight decrease during the 4– 6 pm time period will occur in coastal areas where higher density development is projected.
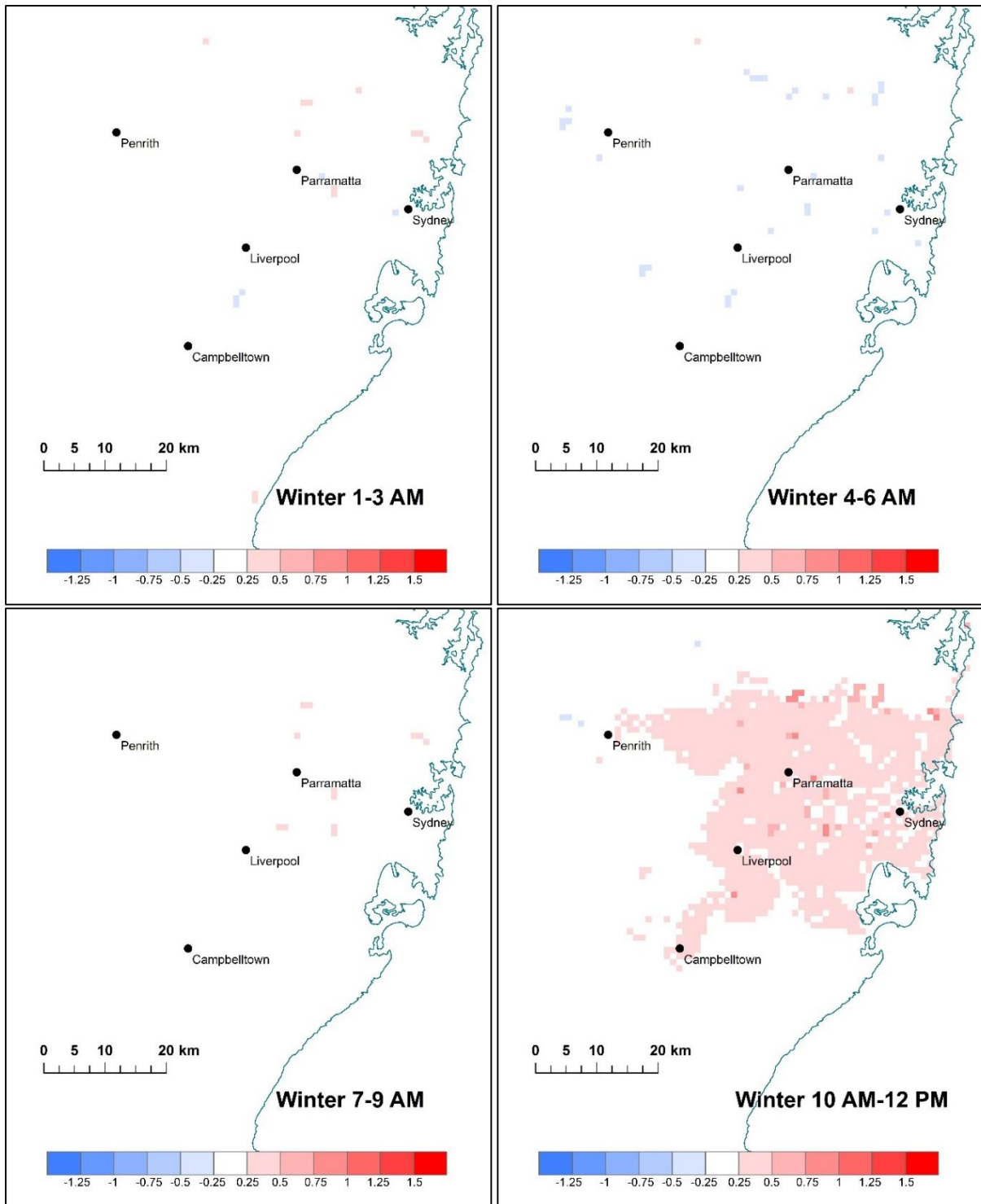
**Figure 17: 3-hourly winter temperature changes between 1 am and 12 pm**

**Figure 18: 3-hourly winter temperature changes between 1 pm and 12 am**

# 4. Discussion

Temperatures for the Sydney GMA are projected to increase by 0.8°C in the near future (2020–2039 compared with the 1990–2009 base climate), based on the ECHAM5 GCM-driven RCM (R3) simulations from the NARCliM project. Aver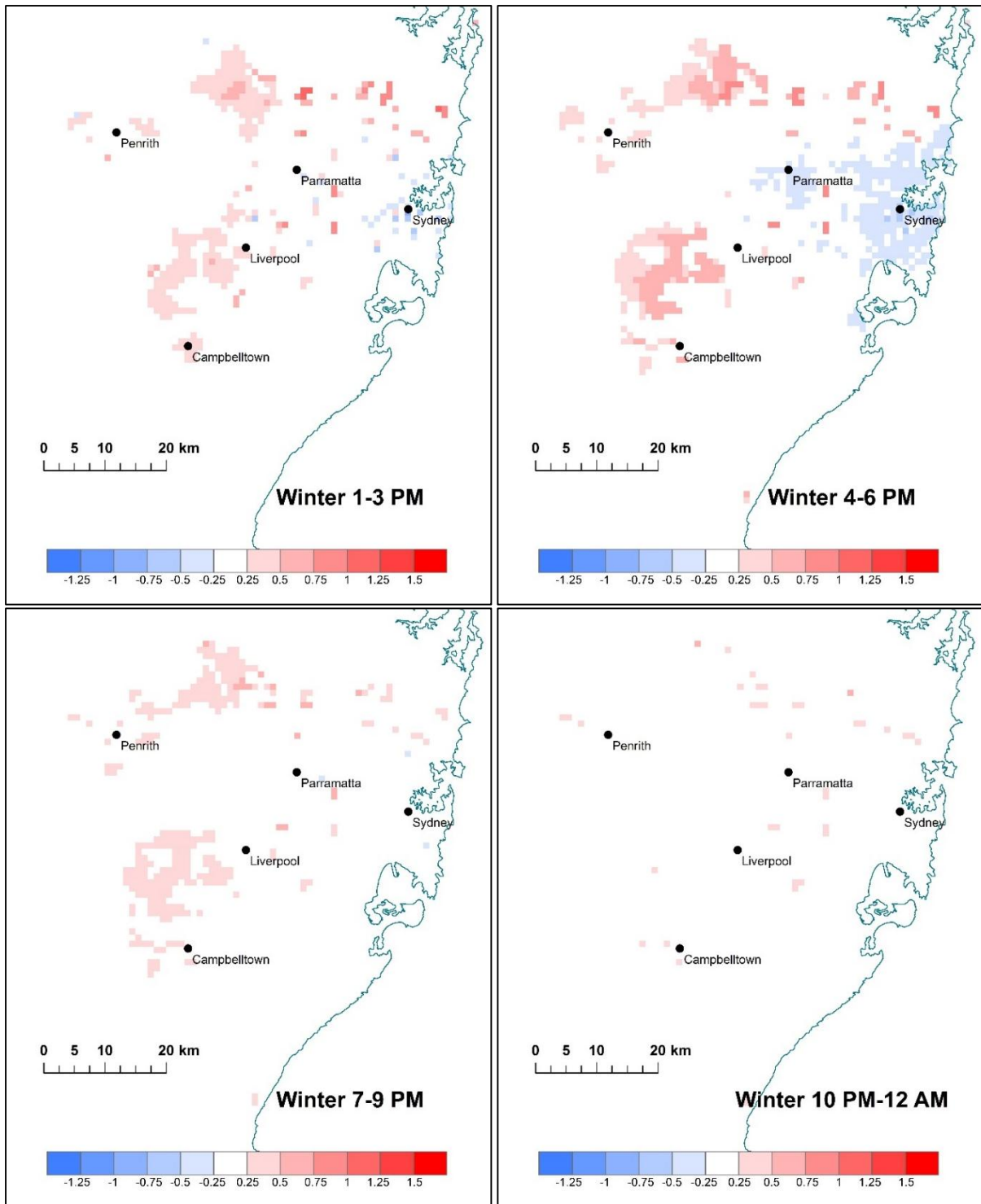age seasonal temperatures are projected to increase by 1.2°C, 0.8°C, 0.5°C and 0.6°C for summer, autumn, winter and spring respectively.

According to findings from this study, future changes to land-use have the potential to enhance temperature increases caused by climate change. The largest temperature increases are projected to occur in areas converted from forest and grasslands to new urban developments. The Priority Growth Areas in the North-West and South-West are expected to undergo this type of land-use change, with the greatest temperature increases therefore projected for these areas. The largest average temperature increases for new urban developments, will occur on summer afternoons and last late into the night.

The influence of land-use changes on temperature is highly dependent on time of day. For example in autumn, a large overall increase in temperature between the hours of 10 am and 12 pm is associated with land-use changes from industrial/commercial to low density urban, with relatively minor implications for the remainder of the day. The pattern of daily influence is also highly dependent on the type of land-use change. For example, in summer between the hours of 1 pm and 9 pm, where land-use changes from grasslands to medium or higher density urban, temperatures are projected to *increase* by 0.5–0.9°C. During the same period of time where land-use changes from high density urban to CBD density urban, temperatures will *decrease* by 0.5°C. Areas which are converted from forest or grasslands to urban are an exception as F→L+, G→L and G→M+ land-use changes have similar patterns.

Temperature changes follow similar patterns throughout the seasons for each type of land-use change. This may be due to the relatively mild climate conditions in the Sydney GMA. However, the magnitude of the temperature change is dependent on the season. The largest temperature changes occur in summer, with the smallest changes seen in winter. Due to the similarity of seasonal patterns it is likely that the magnitude of change is dependent on ambient daily temperature. Therefore projected increases to temperature caused by human induced climate change will likely be exacerbated by temperature changes caused by land-use change.

Increasing urban density in established urban areas did not dramatically increase temperature. On average, increasing urban density from low density urban land-use slightly increased average temperatures. However, increasing urban density from a medium or higher density base decreases average daily temperature. All land-use changes where urban density increased, had increased morning temperatures (7 am–12 pm) throughout the seasons. However, increasing urban density from a medium or higher density base decreased temperatures in each other 3-hourly period. The largest decreases occur in the afternoon (1 pm–6 pm). These decreases are potentially caused by increased building height and the presence of coastal sea breezes. Increased building height will increase shading. Shading reduces the absorption of light and in turn reduces heat emissions from urban materials. Sea breezes are caused by high land temperatures and cool sea temperatures. Sea breezes commence soon after the land temperature exceeds the sea temperature. Additionally, the higher the difference in temperature the stronger the breeze. Thus sea breezes will start earlier and be stronger due to higher morning temperatures caused by increased urban density. The changes to sea breezes will bring cooler temperatures further inland. The changes will also slow temperature build-up. Further investigation is required to better understand the interaction between land-use changes and sea breezes. However, the strength of sea breezes may be exaggerated in the model as many past studies found climate models overestimate land based wind speeds (Xie et al. 2012; Reboredo et al. 2015). Furthermore, the influence of sea breezes is dependent on proximity to the coast, so the location of the land-use change could define how it influences temperature.

# 5. Conclusions

Land-use changes can increase in urban temperatures. Urban development of forests and grasslands in Western Sydney may increase temperatures in 2030 by a similar amount to the changes projected to occur from climate change. The converting of areas in the north-west and south-west of Sydney from forest and grasslands to new urban development more than doubles the temperature changes already projected to occur as a result of climate change. The largest temperature increases in new urban developments are likely occur on summer afternoons and during the night. However, different land-use changes have different effects on temperature during the day. Increasing urban density in medium or higher density urban areas may cause a small decrease in average temperatures. These decreases are potentially related to coastal sea breezes and increased building heights.

The magnitude of the temperature change caused by land-use change is dependent on ambient temperature. Consequently, land-use changes which increase temperature will see the biggest increases on the hottest days. Therefore projected increases to temperature caused by human induced climate change will exacerbate temperature changes caused by land-use change.

The results from this study provide a useful first approximation of future temperatures in the Sydney GMA when land-use change is accounted for. The results from this study can help local planners and policy-makers make informed decisions about urban heat reduction strategies in appropriate areas. They may provide valuable inputs into a range of environmental modelling programs including climatic, ecological and emergency service models. More generally, the results add to our knowledge and understanding of climate change in the Sydney GMA by taking into account future land-use change in the region.

# 6. References

Adams, M & Smith, P 2014, 'A systematic approach to model the influence of the type and density of vegetation cover on urban heat using remote sensing', *Landscape and Urban Planning* **132**, 47–54.

Bureau of Transport Statistics 2012, *BTS Population Forecasts 2006–2046*, Technical Documentation, www.bts.nsw.gov.au/ArticleDocuments/84/TR-2012-10-Population-Forecasts.pdf.aspx

Cardew, R 1996, 'Residential densities in Sydney', *Australian Planner* **33(2)**, 105–113, doi:10.1080/07293682.1996.9657724

Chen, F, Kusaka, H, Tewari, M, Bao, J & Hirakuchi, H 2004, 'Utilizing the coupled WRF/LUL/Urban modeling system with detailed urban classification to simulate the urban heat island phenomena over the Greater Houston area', *Proc. Fifth Conference on Urban Environment*, Vancouver, BC, Canada, American Meteorological Society, paper 9.11.

Chen, F, Kusaka, H, Bornstein, R, Ching, J, Grimmond, C, Grossman-Clarke, S, Loridan, T, Manning, K, Martilli, A, Miao, S, Sailor, D, Salamanca, F, Taha, H, Tewari, M, Wang, X, Wyszogrodzki, A & Zhang, C 2011, 'The integrated WRF/urban modelling system: development, evaluation, and applications to urban environmental problems', *International Journal of Climatology* **31(2)**, 273–288.

Evans, JP, Ji, F, Lee, C, Smith, P, Argüeso, D & Fita, L 2014, 'A regional climate modelling projection ensemble experiment – NARCliM', *Geoscientific Model Development* **7(2)**, 621–629, doi: 10.5194/gmd-7-621-2014.

Feddema, JJ, Oleson, KW, Bonan, GB, Mearns, LO, Buja, LE, Meehl, GA & Washington, WM 2005, 'The importance of land-cover change in simulating future climates', *Science* **310(5754)**, 1674–1678.

Hurley, P 2008, *TAPM V4. User Manual*, CSIRO Marine and Atmospheric Research Group Report No. 5, CSIRO.

IPCC 2013, 'Summary for Policymakers', in Climate Change 2013: The Physical Science Basis, Contribution of Working Group I to the Fifth Assessment Report of the Intergovernmental Panel on Climate Change, TF Stocker, D Qin, G-K Plattner, M Tignor, SK Allen, J Boschung, A Nauels, Y Xia, V Bex & PM Midgley (eds), CambridgeUniversity Press, Cambridge, United Kingdom & New York, USA.

Jackson, T, Feddema, J, Oleson, K, Bonan, G & Bauer, J 2010, 'Parameterization of Urban Characteristics for Global Climate Modeling', *Annals of the Association of American Geographers* **100(4)**, 848–865.

Ji, F, Evans, J, Teng, J, Scorgie, Y, Argueso, D, Di Luca, A & Olson, R 2015, 'Evaluation of long-term precipitation and temperature WRF simulations for southeast Australia' (submitted).

Lipson, M 2014, 'Evaluation and Development of an Australian Urban Climate Model', thesis, University of New South Wales, Faculty of Science School of Biological, Earth and Environmental Sciences.

Loveland T, Reed B, Brown J, Ohlen D, Zhu J, Yang L & Merchant J. 2000. Development of a global land cover characteristics database and IGBP DISCover from 1-km AVHRR data. *International Journal of Remote Sensing* **21**, 1303–1330.

OEH 2012, *The Office of Environment and Heritage Spatial Data Online Access database*, NSW Office of Environment and Heritage, retrieved on 12 October 2015 from http://mapdata.environment.nsw.gov.au/geonetwork/srv/en/main.home

Oke, TR 1988, 'The urban energy balance', *Progress in Physical Geography* **12**, 471–508.

Pielke, RA 2002, *Mesoscale Meteorological Modelling*, Academic Press.

Reboredo, B, Arasa, R & Codina, B 2015, 'Evaluating Sensitivity to Different Options and Parameterizations of a Coupled Air Quality Modelling System over Bogotá, Colombia, Part I: WRF Model Configuration, *Open Journal of Air Pollution* **4**, 47–64, dx.doi.org/10.4236/ojap.2015.42006

Taha, H 1997, 'Urban climates and heat islands: albedo, evapotranspiration, and anthropogenic heat', *Energy and Buildings* **25**, 99–103, doi-10.1016/S0378-7788(96)00999-1

Taylor, A, Parr, A, Johnstone, K, Massey, S, Tranquille, M, Tan, P & Micallef, N 2014, *Population and Household Projections*, retrieved 12 October 2015 from www.planning.nsw.gov.au/projections

Thatcher, M & Hurley, P 2012, 'Simulating Australian Urban Climate in a Mesoscale Atmospheric Numerical Model', *Boundary-Layer Meteorology* **142**, 149–175, doi-10.1007/s10546-011-9663-8

Xie, B, Fung, J, Chan, A & Lau, A 2012, 'Evaluation of nonlocal and local planetary boundary layer schemes in the WRF model', *Journal Of Geophysical Research* **117 (D12)**, doi:10.1029/2011JD017080